

1 **Interleukin-17 regulates neuron-glia communications, inhibitory**
2 **synaptic transmission and neuropathic pain after chemotherapy**

3

4 Hao Luo^{1,2§}, Hui-Zhu Liu^{1§}, Xin Luo², Sangsu Bang², Zi-Long Wang², Gang Chen³,
5 Ru-Rong Ji^{1,2,4*}, Yu-Qiu Zhang^{1,5*}

6

7 ¹State Key Laboratory of Medical Neurobiology and Institutes of Brain Science,
8 Fudan University, Shanghai 200032, China

9 ²Department of Anesthesiology, Duke University Medical Center, Durham, North
10 Carolina 27710

11 ³Key Laboratory of Neuroregeneration of Jiangsu and Ministry of Education,
12 Co-Innovation Center of Neuroregeneration, Nantong University, Nantong, Jiangsu
13 226001, China

14 ⁴Department of Neurobiology, Duke University Medical Center, Durham, North
15 Carolina 27710

16 ⁵Institute of Acupuncture and Moxibustion, Fudan Institute of Integrative Medicine.

17 Number of figures: 8, number of characters: 57,800

18 All the authors have no competing financial interest in this study.

19 [§]HL and HZL contributed equally to this work.

20 *Correspondence should be addressed to Ru-Rong Ji (ru-rong.ji@duke.edu) and

21 Yu-Qiu Zhang (yuqiuzhang@fudan.edu.cn)

22 **Abstract**

23 The proinflammatory cytokine Interleukin-17 (IL-17) is produced mainly by Th17
24 cells and has been implicated in pain regulation. However, synaptic mechanisms by
25 which IL-17 regulates pain transmission are unknown. Here we report that
26 glia-produced IL-17 suppresses inhibitory synaptic transmission in spinal cord pain
27 circuit and drives chemotherapy-induced neuropathic pain. We observed respective
28 expression of IL-17 and its receptor IL-17R in spinal cord astrocytes and neurons.
29 Patch clamp recording in spinal cord slices revealed that IL-17 not only enhanced
30 EPSCs but also suppressed IPSCs and GABA-induced currents in lamina II_o
31 somatostatin-expressing neurons. Spinal IL-17 was upregulated after paclitaxel
32 treatment, and intrathecal IL-17R blockade reduced paclitaxel-induced neuropathic
33 pain. In dorsal root ganglia, respective IL-17 and IL-17R expression in satellite glial
34 cells and neurons was sufficient and required for inducing neuronal hyperexcitability
35 after paclitaxel. Together, our data show that IL-17/IL-17R mediate both central and
36 peripheral neuron-glia interactions in chemotherapy-induced peripheral neuropathy.

37 **Keywords:** Interleukin-17; chemotherapy-induced peripheral neuropathy; dorsal root
38 ganglia (DRG), inhibitory postsynaptic synaptic currents (IPSCs);
39 somatostatin-expressing neurons; spinal cord

40

41

42

43 **Introduction**

44 Pro-inflammatory cytokines such as TNF- α , IL-1 β , and IL-18 play important roles in
45 the pathogenesis of chronic pain (Sommer, 1999, Zelenka et al., 2005, Milligan et al.,
46 2001, Yang et al., 2015, Miyoshi et al., 2008, Sweitzer et al., 1999, Guo et al., 2007).
47 Increasing evidence suggests that glial cells such as microglia and astrocytes are
48 activated in pathological pain conditions to produce these pro-inflammatory cytokines.
49 Especially, these cytokines act as neuromodulators and regulate pain via neuron-glia
50 interactions (Ji et al., 2013, Grace et al., 2014). Compared to TNF and IL-1 β , and IL-6,
51 much less is known about the role of IL-17 in pain regulation. IL-17, referred to as
52 IL-17A in the literature, is a proinflammatory cytokine produced by Th17 cells
53 (Miossec and Kolls, 2012, Korn et al., 2009). The IL-17 family consists of six ligands
54 (IL-17A–F) and five receptors (IL-17RA–IL-17RE) in mammals, (Gaffen, 2009).
55 IL-17 was shown to regulate rheumatoid arthritis and immune responses by increasing
56 the production of IL-6 and IL-8(Hwang et al., 2004). Binding of IL-17 to its receptor
57 (IL-17RA) induces the activation of nuclear factor- κ B (NF- κ B) via ACT1 and TNF
58 receptor-associated factor 6 (TRAF6) in rheumatoid arthritis(Hot and Miossec, 2011).
59 However, little is known about non-transcriptional regulation of IL-17.
60 Recently, IL-17 was found to regulate inflammatory responses associated with
61 neuropathic pain induced by nerve injury. IL-17 levels are upregulated in the injured
62 nerves in neuropathic pain models(Noma et al., 2011, Kleinschnitz et al., 2006).
63 IL-17 receptor (IL-17R) was detected in most neurons in dorsal root ganglion (DRG)

64 as well as in cultured DRG neurons (Segond von Banchet et al., 2013, Richter et al.,
65 2012). IL-17A-deficient mice showed less mechanical hyperalgesia compared to
66 normal mice after zymosan injection (Segond von Banchet et al., 2013) or partial
67 ligation of the sciatic nerve (Kim and Moalem-Taylor, 2011). Further, Intraplantar
68 (Kim and Moalem-Taylor, 2011, McNamee et al., 2011) or intra-knee (Pinto et al.,
69 2010) injection of recombinant IL-17 is sufficient to induce hyperalgesia. Notably,
70 IL-17 can also be produced by spinal cord astrocytes, and astrocytic IL-17 may play a
71 role in inflammatory pain (Meng et al., 2013). A recent study found that
72 physiological levels of IL-17 can act directly on interneurons to increase their
73 responsiveness to presynaptic input (Chen et al., 2017). Despite these previous studies,
74 it remains elusive how IL-17 modulates spinal synaptic transmission in the pain
75 circuit.

76 Chemotherapy-induced peripheral neuropathy (CIPN) is a common dose-limiting
77 adverse effect and results in high incidence of neuropathic pain (Sisignano et al.,
78 2014). There is evidence that spinal astrocytes but not microglia play an important
79 role in the pathogenesis of paclitaxel-induced neuropathy (Zhang et al., 2012a, Luo et
80 al., 2017). CIPN enhances excitability of primary sensory neurons associated with
81 altered gene expression of neuronal ion channels. (Zhang and Dougherty, 2014) and
82 also increases excitatory synaptic transmission in spinal cord substantia gelatinosa
83 neurons (Li et al., 2015a).

84 The somatostatin-positive (SOM⁺) neurons are a subset of interneurons in the dorsal

85 horn. These neurons are predominantly excitatory and express the vesicular glutamate
86 transporter VGLUT₂, a marker for glutamatergic excitatory neurons (Duan et al., 2018,
87 Xie et al., 2018). Recently, Duan et al. demonstrate that SOM⁺ neurons are required to
88 sense mechanical pain (Duan et al., 2014b). These neurons form a pain circuit by
89 receiving input from capsaicin-sensitive C-fibers and sending output to lamina I
90 projection neurons (Todd, 2010, Braz et al., 2014). SOM⁺ also receive input from
91 inhibitory neurons (Duan et al., 2014b). Furthermore, these neurons exhibit
92 remarkable plastic changes after inflammation and nerve injury and respond to
93 inflammatory mediators (Park et al., 2011, Xie et al., 2018, Xu et al., 2010). Here,
94 we investigated how IL-17 and IL-17R modulate excitatory and inhibitory synaptic
95 transmission of SOM⁺ excitatory neurons in the normal and pathological pain
96 conditions and further tested the involvement of IL-17/IL-17R signaling in
97 paclitaxel-induced neuropathic pain model. Our findings demonstrate that IL-17
98 signaling contributes to paclitaxel-induced mechanical allodynia and dysregulations
99 of excitatory and inhibitory synaptic transmission in spinal SOM⁺ neurons. Moreover,
100 we reveal new insights into neuron-glia interactions in the spinal cord and DRG, by
101 which IL-17 produced by astroglia or satellite glia enhance neuronal activities and
102 excitability to promote neuropathic pain.

103

104

105

106 **Methods**

107 **Animals.** Most experiments were performed on adult C57BL/6 mice (8-10 weeks,
108 male, purchased from Charles River). Some electrophysiology experiments were
109 conducted in transgenic C57BL/6 mice (5-6 weeks). These mice express tdTomato
110 fluorescence in somatostatin (SOM⁺) neurons, after Som-Cre mice were crossed with
111 tdTomato Cre-reporter mice (Rosa26-floxed stop tdTomato mice), both from Jackson
112 Laboratory, to generate conditional transgenic mice that express tdTomato in SOM⁺
113 neurons. All the animal procedures were approved by the Institutional Animal Care &
114 Use Committee (IACUC) of Duke University and Fudan University.

115 Intraperitoneal (i.p.) injection of paclitaxel (PAX, 6 mg/kg for a single injection or 2
116 mg/kg for multiple injections at days 0, 2, 4, and 6) was given to generate
117 chemotherapy-associated neuropathic pain (20). 7 days following the injection, spinal
118 dorsal horns and CSF were collected.

119 **Reagents and drug injection.** We purchased the recombinant mouse IL-17A protein
120 (R&D System Inc., MN, USA., 421-ML), mouse IL-17 receptor A (IL-17 RA or
121 IL-17R) antibody (R&D System Inc., MN, USA., MAB4481) and control IgG (R&D
122 Systems Inc., MN, USA.). GABA, and glycine were obtained from Sigma-Aldrich.
123 IL-17 was prepared as 1000 fold stock solution in 4 mM HCl and finally used at the
124 concentration of 10 ng/mL. All compounds were prepared in artificial cerebrospinal
125 fluid (ASCF). Picrotoxin, strychnine, AP-5 or CNQX were purchased from Sigma
126 Company.

127 IL-17 or vehicle was delivered to CSF space between L5 and L6 vertebrae via a spinal
128 cord puncture, which is made by a 30 Gage needle. Before puncture, the mice' heads
129 were covered by a piece of cloth. Ten microliters of solution were injected with a
130 microsyringe. A successful spinal puncture was confirmed by a brisk tail-flick.

131 **ELISA.** ELISA was performed using CSF and spinal cord tissues. The tissues were
132 homogenized in a lysis buffer containing protease and phosphatase inhibitors (Sigma
133 Chemical Co), and tissue samples were centrifuged (12,500×g for 10 min) to obtain
134 extract proteins. CSF was collected from the cisterna magna . For each ELISA assay,
135 50 µg proteins, or 5 µL of CSF were used. ELISA was conducted according to
136 manufacturer's instructions (R&D Systems Inc., MN, USA., Cat# PM1700) and the
137 standard curve was included in each experiment..

138 **Behavior.** Animals were habituated to the testing environment for at least 2 days
139 before the testing. Animals were kept in boxes on an elevated metal mesh floor.
140 Mechanical allodynia was assessed by measuring paw withdrawal thresholds in
141 response to a series of von Frey hairs (0.16-2.0 g, Stoelting Company). The
142 withdrawal threshold was determined using the Dixon's up-down method.

143 **Immunohistochemistry.** Mice were deeply anesthetized with urethane and were
144 transcardially perfused with normal saline followed by 4% paraformaldehyde in 0.1
145 M PB. The L4–L6 segments of the spinal cord were removed and postfixed for 24 h at
146 4 °C, and then dehydrated in gradient sucrose at 4 °C. Transverse spinal cord sections
147 (30 µm) were cut on a cryostat (model 1900, Leica). The sections were blocked with

148 PBS containing 10% donkey serum and 0.3% Triton X-100 for 2 h at RT and then
149 incubated for 48 h at 4 °C with a mixture of rabbit anti-IL-17 (1:50) and mouse
150 anti-NeuN (1:2000)/rabbit anti-IBA-1 (1:500)/mouse anti-GFAP (1:2000) antibodies,
151 or rabbit anti-IL-17R (1:200) and anti-NeuN/GFAP/IBA-1. The sections were then
152 incubated with a mixture of FITC-conjugated secondary antibodies (1:200; Jackson
153 ImmunoResearch) for 2h at RT. Negative control was included by the omission of the
154 primary antibodies. The stained sections were observed and the images captured with
155 a confocal laser-scanning microscope (model FV1000, Olympus).

156 **Preparation of spinal cord slices and whole-cell patch-clamp recordings.** The
157 L4–L5 lumbar spinal cord segment was rapidly removed under urethane anesthesia
158 (1.5 - 2.0 g/kg, i.p.) and transferred to ice-cold cutting ACSF containing (in mM)
159 NaCl 80, KCl 2.5, NaH₂PO₄ 1.25, CaCl₂ 0.5, MgCl₂ 3.5, NaHCO₃ 25, sucrose 75,
160 ascorbate 1.3, sodium pyruvate 3.0, oxygenated with 95% O₂ and 5% CO₂, pH 7.4.
161 Transverse slices (450 μm) were cut on a vibrating blade microtome (Leica VT1200 S)
162 and incubated in recording ACSF oxygenated with 95% O₂ and 5% CO₂ for at least 1
163 h at 32 °C before recording. Slices were then transferred to the chamber and perfused
164 with recording solution at a rate of 3 ml/min at RT. The recording ACSF contains the
165 following (in mM): NaCl 125, KCl 2.5, CaCl₂ 2, MgCl₂ 1, NaH₂PO₄ 1.25, NaHCO₃
166 26, D -glucose 25.

167 The whole-cell patch clamp recordings were performed in lamina IIo SOM⁺ neurons
168 in voltage-clamp mode. Patch pipettes (5–10 MΩ) were made of borosilicate glass on

169 a horizontal micropipette puller (P-97, Sutter Instruments) analysis. For spontaneous
170 excitatory postsynaptic currents (sEPSCs) recordings, pipette solution contained (in
171 mM): potassium gluconate 120, KCl 20, MgCl₂ 2, Na₂ATP 2, NaGTP 0.5, HEPES 20,
172 EGTA 0.5, adjusted to pH 7.3 with KOH. For spontaneous inhibitory postsynaptic
173 currents (sIPSCs), pipette solution contained (in mM): CsCl 130, NaCl 9, MgCl₂ 1,
174 EGTA 10, HEPES 10, adjusted to pH 7.3 with CsOH. After establishing the
175 whole-cell configuration, neurons were held at -70 mV to record sEPSCs in the
176 presence of 100 μM picrotoxin and 2 μM strychnine. Signals were filtered at 2 kHz
177 and digitized at 5 kHz. NMDA receptor mediated EPSC was evoked by electrical
178 stimulation of Lissauer's tract, using a low Mg²⁺ recording ACSF (2.5 mM Ca²⁺, 0.25
179 mM Mg²⁺) with CNQX (10 μM), BMI (10 μM) and strychnine (2 μM). A constant
180 current pulse (0.3–0.5mA) at 0.05 Hz was applied to the Lissauer's tract to evoke
181 EPSC. When recording NMDA-EPSCs, a holding potential at -40 mV was used as
182 indicated. GABA current and glycine current were induced by 100 μM GABA and 1
183 mM glycine, respectively. Data were collected with pClamp 10.1 software and
184 analyzed with Mini Analysis and Clampfit.

185 **Whole-cell patch clamp recordings in dissociated mouse DRG neurons.** DRGs
186 were aseptically removed from 5-8 week-old mice and digested with collagenase (0.2
187 mg/ml, Roche)/dispase-II (3 mg/ml, Roche) for 120 min. Cells were placed on glass
188 cover slips coated with poly-D-lysine and grown in a neurobasal defined medium (10%
189 fetal bovine serum and 2% B27 supplement) at 37 °C with 5% CO₂ for 24 h before

190 experiments.

191 **Human DRG neuron cultures and whole-cell patch clamp recordings.**

192 Non-diseased human DRGs were obtained from donors through National Disease
193 Research Interchange (NDRI) with permission from the Duke University Institutional
194 Review Board (IRB). Postmortem L3–L5 DRGs were dissected from donors and
195 delivered in ice-cold culture medium to the laboratory at Duke University within
196 24–72 h of the donor's death. Upon the delivery, DRGs were rapidly dissected from
197 nerve roots and minced in a calcium-free HBSS (Gibco). Human DRG cultures were
198 prepared as previously reported (Han et al., 2016, Chang et al., 2018). DRGs were
199 digested at 37 °C in a humidified O₂ incubator for 120 min with collagenase Type II
200 (Worthington, 290 units/mg, 12 mg/ml final concentration) and dispase II (Roche, 1
201 unit/mg, 20 mg/ml) in PBS with 10 mM HEPES, pH adjusted to 7.4 with NaOH.
202 hDRGs were mechanically dissociated using fire-polished pipettes, filtered through a
203 100 µm nylon mesh and centrifuged for 5 min (500g). The DRG cell pellet was
204 resuspended, plated on 0.5 mg/ml poly-D-lysine-coated glass coverslips. DRG
205 cultures were grown in Neurobasal medium supplemented with 10% FBS, 2% B-27
206 supplement, and 1% penicillin/streptomycin.

207 Whole-cell patch-clamp recordings in small-diameter (<55 µm) human DRG neurons
208 were conducted at room temperature. We used an Axopatch-200B amplifier with a
209 Digidata 1440A (Axon Instruments) to measure action potentials and resting
210 membrane potential. The patch pipettes were pulled from borosilicate capillaries

211 (World Precision Instruments, Inc.). The resistance of the pipettes was 3-4 M Ω , when
212 filled with the pipette solution. The recording chamber (300 μ l) was continuously
213 superfused at the flow rate of 1-2 ml/min. Series resistance was compensated (> 80%)
214 and leak subtraction was performed. Data were low-pass-filtered at 2 KHz and
215 sampled at 10 KHz. The pClamp10.6 (Axon Instruments) software were used during
216 experiments and Clampfit 10.6 were used for analysis. The pipette solution contained
217 (in mM): potassium gluconate 126, NaCl 10, MgCl₂ 1, EGTA 10, Na-ATP 2 and
218 Mg-GTP 0.1, adjusted to pH 7.3 with KOH. The external solution contained: NaCl
219 140, KCl 5, CaCl₂ 2, MgCl₂ 1, HEPES 10, glucose 10, adjusted to pH 7.4 with NaOH.
220 In current-clamp experiments, the action potentials were evoked by a current injection.
221 The resting membrane potential was measured without a current injection.

222 **Data analysis and statistics.** All data were expressed as mean \pm S.E.M. ELISA and
223 behavioral data were analyzed using Student's t-test (two groups) or two-way
224 ANOVA followed by post-hoc Bonferroni test. Electrophysiological data were tested
225 using two-way ANOVA followed by post-hoc Bonferroni test or two-tailed paired
226 t-test. The criterion for statistical significance was $p < 0.05$.

227

228

229

230

231 **Results**

232 *Distinct cellular localization of IL-17 and IL-17R in spinal dorsal horn.* As the first
233 step to define the role of IL-17 and IL-17R in regulating spinal cord synaptic
234 transmission and CIPN, we examined cellular location of IL-17 and IL-17R in spinal
235 cord. Double immunofluorescence labeling demonstrated that IL-17 immunoreactivity
236 (IR) was primarily colocalized with the astrocyte marker GFAP but not with the
237 neuronal marker NeuN or the microglia marker IBA1 in spinal dorsal horn (Fig.
238 1A-C). Interestingly, IL-17R-IR showed distinct expression pattern. IL-17 receptor
239 was predominantly colocalized with NeuN but not with GFAP or IBA1 in the spinal
240 cord dorsal horn (Fig. 2A-C). The data indicate that IL-17 is expressed by astrocytes
241 but its receptor is expressed by neurons in spinal cord. Notably, the expression of
242 IL-17 and IL-17R was enriched in the superficial dorsal horn, where nociceptive input
243 (C- and A δ -afferents (Basbaum et al., 2009). These unique expression patterns of the
244 ligand-receptor pair provide an anatomical base for IL-17 to mediate neuron-glia
245 interaction in the spinal cord pain pathway.

246 *IL-17 enhances excitatory synaptic transmission and potentiates NMDA-mediated*
247 *eEPSC in spinal cord slices.* SOM⁺ neurons are excitatory interneurons and
248 indispensable for mechanical pain (Duan et al., 2014a, Duan et al., 2018). These
249 neurons also exhibit marked synaptic plasticity in pathological pain conditions (Xie et
250 al., 2018, Xu et al., 2013). We first recorded spontaneous EPSCs (sEPSCs) in outer
251 lamina II (II_o) SOM⁺ neurons in isolated spinal cord slices of SOM-tdTomato mice

252 (Fig. 3A). Acute perfusion of IL-17, at a low concentration (10 ng/mL, 3 min),
253 induced a rapid and significant increase in 8 out of 10 neurons in the frequency of
254 sEPSCs (Fig. 3 B, C, E, $p=0.0003$), suggesting a possible presynaptic mechanism of
255 IL-17 to enhance glutamate releases. Notably, IL-17 produced a 57% increase in
256 sEPSC frequency. Because excitatory synaptic transmission is mainly mediated by
257 AMPA and NMDA receptors (AMPA and NMDAR) and NMDAR is critical for
258 spinal cord synaptic plasticity and pathogenesis of pain (Woolf and Salter, 2000), we
259 further examined the effects of IL-17 on NMDAR-EPSC evoked by dorsal root entry
260 zoon (LT) stimulation. The amplitude of NMDAR-EPSC was also significantly
261 increased by IL-17 (Fig. 3 G, H, 37%, $p=0.0077$), suggesting a positive regulation of
262 excitatory synaptic transmission by IL-17.

263 ***IL-17 decreases the inhibitory control of SOM⁺ neurons and suppresses GABA-***
264 ***induced currents.*** SOM⁺ excitatory neurons receive inhibitory input from inhibitory
265 neuron (Duan et al., 2014b). We next recorded spontaneous IPSC (sIPSCs) in lamina
266 II_o SOM⁺ neurons by using a pipette solution containing Cs²⁺. After exposure of
267 spinal cord slice to IL-17 (10 ng/mL) for 3 min, most neurons (7 out 10) responded to
268 IL-17. IL-17 produced a significant decrease of sIPSCs in both frequency (Fig. 4A, B,
269 E, $p=0.0039$) and amplitude (Fig. 4C, F, $p=0.0019$). Because inhibitory synaptic
270 transmission in the spinal cord is mediated by GABA and glycine, two major
271 inhibitory neurotransmitters (Todd, 2010), we further assessed if IL-17 would also
272 alter GABA and glycine evoked currents in lamina II_o SOM⁺ neurons. Bath

273 application of GABA (100 μ M) and glycine (1 mM) induce marked inward currents.
274 Interestingly, acute application of IL-17 (10 ng/ml) only inhibited GABA-induced
275 current (Fig. 4D, I, $P=0.0016$) but had not effect on glycine-induced current in spinal
276 SOM^+ neurons (Fig. 4H, J, $P=0.2540$), suggesting a specific regulation of IL-17 on
277 GABAR-mediated inhibitory synaptic transmission.

278 *Up-regulation of endogenous IL-17 and IL-17R regulates synaptic plasticity in*
279 *paclitaxel-treated mice.* We first tested whether paclitaxel alters IL-17 levels in CSF
280 and spinal cord. The CSF and spinal cord dorsal horns were collected from mice with
281 confirmed mechanical allodynia at day 7 after paclitaxel treatment. ELISA analysis
282 demonstrated significant increases in IL-17 levels in the spinal cord dorsal horn and
283 CSF samples of paclitaxel-treated mice vs. vehicle-treated mice (Fig. 5A,B,
284 $p=0.0092$). Also, we found that majority of spinal SOM^+ neurons express IL-17R,
285 providing an anatomical basis for IL-17 to directly regulate the activities of SOM^+
286 neurons (Fig. 5 C).

287 On the basis of these results, we postulated that IL-17 upregulation after
288 chemotherapy contributes to spinal cord synaptic plasticity (i.e. central sensitization),
289 a driving force of pathological pain (Ji, 2017). We measured the frequency and
290 amplitude of sEPSCs or sIPSCs of spinal SOM^+ neurons in paclitaxel-treated mice
291 and tested the involvement of endogenous IL-17 in synaptic plasticity after CIPN.
292 Blocking IL-17R with a neutralizing antibody resulted in opposite changes in
293 excitatory and inhibitory synaptic transmission in lamina II_o SOM^+ neurons of

294 paclitaxel-treated animals: a decrease in frequency of sEPSCs (Fig. 5D, E, F,
295 $p=0.0019$) but an increase in sIPSC frequency (Fig. 5G, H, $p=0.0004$) and sIPSC
296 amplitude (Fig. 5I, $p=0.0384$) However, control IgG had no effects on sIPSC (Fig.
297 5G). Thus, endogenous IL-17 is involved in modulating excitatory and inhibitory
298 synaptic transmission in spinal SOM⁺ neurons via IL-17R after paclitaxel treatment,
299 suggesting a role of the IL-17-IL-17R pathway in CIPN.

300 ***IL-17 increases the excitability of small-sized mouse and human DRG neurons.***

301 Immunostaining revealed that IL-17R is expressed by small-sized mouse DRG
302 neurons, and some of them bind IB4 (Fig. 6A). This is consistent with a previous
303 report that IL-17RA is localized in majority of rat DRG neurons (Richter et al., 2012).
304 In contrast, IL-17 expression was observed in satellite glial cells that express
305 glutamine synthetase (GS, Supplementary Figure 1). This respective expression of
306 IL-17 and IL-17R in glia and neurons in the DRG is similar to that observed in the
307 spinal cord, suggesting that IL-17 and IL-17R can mediate neuron-glia interactions
308 both in the central and peripheral nervous system.

309 To determine a role of IL-17 in regulating the excitability of DRG neurons, we tested
310 the effects of IL-17 on dissociated small-sized mouse DRG neurons (< 25 μm in
311 diameter) using whole-cell patch clamp recordings. Acute application of IL-17 (10
312 ng/ml) to mouse DRG neurons in vitro induced spontaneous discharge and bursts of
313 action potentials in some DRG neurons (Fig. 6 B). Also, IL-17 significantly
314 depolarized the resting membrane potential (Fig. 6 C, $p=0.0001$) and significantly

315 decreased rheobase (Fig. 6 D, $p=0.0068$). IL-17 bath application also increased
316 numbers of action potential discharges to suprathreshold current injection (Fig. 6 E, F).
317 Therefore, IL-17 increases excitability of nociceptive neurons by altering rheobase
318 and resting membrane potential in nociceptive neurons, leading to enhanced
319 discharges of action potentials.

320 To enhance translational potential of this study, we also examined the action of IL-17
321 in human DRG neurons. An example of small-sized human DRG neuron from
322 disease-free donors is shown in Figure 6G. Like mouse DRG neurons, human DRG
323 neurons showed spontaneous action potentials and increased AP firing number during
324 acute application of human IL-17 (10 ng/ml, Fig. 6 H-J). Also, IL-17 caused
325 significant depolarization in the resting membrane potential on human DRG neurons
326 ($p = 0.016$, Fig. 6K). These findings in isolated mouse and human DRG neurons show
327 that IL-17 has the potential to directly increase the excitability of primary afferent
328 neurons.

329 ***IL-17R is required for hyperexcitability of mouse DRG neurons after paclitaxel***
330 ***chemotherapy.*** Paclitaxel was shown to increase responsiveness and excitability of
331 mouse and human DRG neurons (Chang et al., 2017, Li et al., 2015b). We compared
332 the number of APs evoked by a 600-ms current injection through intracellular
333 electrode in mouse DRG neurons and tested the effects of paclitaxel after bath
334 application (1 μ M, 2 h). Only neurons that showed more than one AP to the
335 stimulation were included in the analysis. Paclitaxel increased the AP firing numbers

336 in small sized neurons compared with the vehicle-treated neurons (Fig. 7A, B).
337 Strikingly, this excitability increase was suppressed by IL-17RA antibody, as
338 compared with control IgG (Fig. 7 C, D). This result implies a direct regulation of
339 neuronal hyperexcitability by IL-17R after chemotherapy.

340 ***IL-17 and IL-17R contribute to mechanical hypersensitivity after chemotherapy.*** To
341 test a central role of IL-17 in pain modulation, we compared mechanical pain
342 thresholds of mice following intrathecal injection of IL-17 and vehicle. Spinal
343 injection of low dose of IL-17 (50 ng, i.t.) resulted in a transient reduction in paw
344 withdrawal threshold (PWT) in 1 h, but the mechanical allodynia recovered in 2 h
345 (Fig. 8A). A high dose of IL-17 (100 ng, i.t.) caused a more persistent reduction in
346 PWT for 3 h, recovering after 5 h (Fig. 8A). These data suggest that IL-17 is sufficient
347 to induce pain hypersensitivity in naïve animals.

348 Finally, we investigated the contribution of IL-17R to chemotherapy-evoked
349 neuropathic pain. A single injection of paclitaxel (6 mg/kg, i.p.) evoked a remarkable
350 reduction in PWT on day 7, which was reversed by IL-17RA antibody (10 µg, i.t.), in
351 a dose-dependent manner. Intrathecal injection of control IgG (10 µg) produced no
352 changes in PWT (Fig. 8B). The results indicate that IL-17R is required for
353 maintaining chemotherapy-induced neuropathic pain.

354

355

356 **Discussion**

357 We have provided new insights into how IL-17 promotes chemotherapy-induced
358 neuropathic pain. Our results show that IL-17 and IL-17R regulate neuropathic pain
359 via multiple mechanisms, including neuron-glia interactions, central sensitization,
360 and peripheral sensitization (Supplemental Figures 1 and 2). In the spinal cord, IL-17
361 increases NMDA receptor-mediated currents and facilitates excitatory synaptic
362 transmission. In particular, IL-17 suppresses inhibitory synaptic transmission by
363 inhibiting GABA receptor-mediated currents. In the DRG, IL-17 increases neuronal
364 excitability and IL-17R contributes to paclitaxel-induced nociceptor hyperactivity.

365 *IL-17 and IL-17R mediate neuron-glia interactions both in the central and*
366 *peripheral nervous system.* Recent progress has demonstrated critical roles of spinal
367 glial cells in driving chronic pain via production of proinflammatory cytokines and
368 neuron-glia interactions (Ji et al., 2016, McMahon and Malcangio, 2009, Ren and
369 Dubner, 2010, Gosselin et al., 2010).

370 Microglia and astrocytes play different roles in different pain conditions, such as
371 CIPN. Paclitaxel was shown to induce astrocyte activation but not microglia
372 activation in the spinal cord (Zhang et al., 2012b). Activation of p38 MAP kinase in
373 spinal microglia contributes to neuropathic pain after nerve trauma and cancer pain
374 (Jin et al., 2003, Yang et al., 2015). However, spinal inhibition of p38 MAP kinase
375 fails to affect chemotherapy-induced mechanical allodynia (Luo et al., 2017). Our
376 results also highlight a role of astrocytes in CIPN. IL-17 is a T cell-derived cytokine,

377 but we found IL-17 immunoreactivity exclusively in GFAP-expressing astrocytes. In
378 contrast, IL-17R was primarily expressed in spinal cord neurons including SOM⁺
379 neurons. This unique localization of IL-17 and IL-17R offers a cellular basis for
380 astroglia-neuro interaction in pain regulation. In parallel, we observed respective
381 expression of IL-17 and IL-17R in satellite glial cells and neurons in mouse DRG.
382 Thus, IL-17/IL-17R signaling could promote both central sensitization and peripheral
383 sensitization via neuron-glia interactions in the CNS and PNS.

384 ***IL-17 and IL-17R modulate excitatory synaptic transmission in the spinal cord pain***
385 ***circuit.*** Enhanced excitatory synaptic transmission has been shown in spinal cord
386 neurons including SOM⁺ neurons in various pathological pain conditions (Chen et al.,
387 2015, Yang et al., 2015). Our data indicates that IL-17 is both sufficient and required
388 for inducing this synaptic plasticity. Exogenous IL-17 rapidly increased EPSC in
389 spinal cord slices from naïve animals. Spinal cord slice from paclitaxel-treated
390 animals exhibited an increase in EPSCs, which was suppressed by IL-17R antibody,
391 suggesting an endogenous role of IL-17 in CIPN. Mechanistically, IL-17 acutely
392 enhanced amplitude of NMDA evoked currents following dorsal root stimulation,
393 suggesting that IL-17 increases NMDAR activity via rapid post-translational
394 regulation. This is consistent with the previous report that IL-17 acts on spinal
395 nociceptive neurons co-expressing IL-17R and NR1 to modulate pain (Meng et al.,
396 2013). NMDAR plays a critical role in the induction and maintenance of central
397 sensitization during persistent pain conditions (Woolf and Thompson, 1991, South et

398 al., 2003). It remains to be investigated how IL-17 modulates NMDAR activity. It is
399 possible that IL-17 activates protein kinases such as extracellular-regulated kinase
400 (ERK) and protein kinase C to enhance NMDAR activation and neuronal excitability
401 (Hu and Gereau, 2003). For example, TNF- α increases NMDA currents in spinal cord
402 lamina II_o neurons via ERK phosphorylation (Xu et al., 2010). Thus, IL-17 plays a
403 role in spinal pain modulation in part via NMDAR-mediated glutamatergic synaptic
404 transmission.

405 ***Modulation of inhibitory synaptic transmission by IL-17 and IL-17R.*** One of the
406 most interesting findings of this study is profound suppression of inhibitory synaptic
407 transmission in lamina II_o SOM⁺ neurons. Disinhibition, i.e., loss of inhibitory
408 synaptic transmission is emerging as a key mechanism of neuropathic pain (Coull et
409 al., 2003, Zeilhofer et al., 2012a, Lu et al., 2013). Removal of spinal inhibition,
410 especially presynaptic GABAergic inhibition, not only reduces the fidelity of normal
411 sensory processing but also provokes symptoms very much reminiscent of
412 inflammatory and neuropathic chronic pain syndromes (Zeilhofer et al., 2012b,
413 Takazawa et al., 2017, Chen et al., 2014). Our study shows that exogenous IL-17
414 rapidly (within a minute) and drastically decreased the frequency and amplitude of
415 sIPSC. Mechanistically, IL-17 specially suppressed GABA but not glycine induced
416 currents. Although TNF- α and IL-1 β were also shown to regulate inhibitory synaptic
417 transmission in spinal cord neurons (Kawasaki et al., 2008, Zhang et al., 2010, Chirila
418 et al., 2014), they act on different pain circuits in the spinal cord. Multiple

419 mechanisms have been implicated in disinhibition in pathological pain (Zeilhofer et
420 al., 2012b) . Our data suggest that IL-17 can elicit a very rapid loss of inhibition to
421 open the spinal gate, which allows low-threshold mechanical stimuli to activate pain
422 transmission neurons as predicted by the “Gate control theory” (Melzack and Wall,
423 1965, Wall, 1978). Majority of SOM⁺ excitatory neurons distribute in lamina II. These
424 neurons not only receive an excitatory input from C- , A β - and A δ -fibers, but also
425 receive an inhibitory control from inhibitory neurons (Duan et al., 2014b). Thus IL-17
426 may induce pain via distinct synaptic mechanisms either by increasing excitatory
427 synaptic transmission or by decreasing inhibition control of SOM⁺ excitatory neurons.
428 Our working hypothesis is illustrated in Supplementary Fig. 2

429 ***Modulation of DRG neuronal excitability after chemotherapy.*** Paclitaxel (Taxol)
430 is a widely used chemotherapeutic agent producing a neuropathy characterized by
431 pronounced impairment of function in A-beta myelinated fibers, intermediate
432 impairment of A-delta myelinated fibers, a relative sparing of C-fibers (Dougherty et
433 al., 2004) and mechanical hypersensitivity (hyperalgesia and allodynia) (Polomano et
434 al., 2001, Fossiez et al., 1996). Mechanical allodynia after paclitaxel is in part
435 mediated by A-beta fibers (Xu et al., 2015). Paclitaxel increases excitability of DRG
436 neurons via regulating the expression and function of ion channels such as TRPV1,
437 TRPV4, HCN1, Nav1.7, leading to increased excitatory synaptic input to spinal
438 cord SG neurons (Zhang and Dougherty, 2014, Li et al., 2015a, Chang et al., 2018).
439 Peripheral mechanisms of pain modulation by IL-17 have been investigated. For

440 example, IL-17 sensitizes joint nociceptors to mechanical stimuli to facilitate arthritic
441 pain (Richter et al., 2012). It was also reported that neuronal IL-17R regulates
442 mechanical but not thermal hyperalgesia by upregulation of TRPV4 but not TRPV1 in
443 DRG neurons (Segond von Banchet et al., 2013). We observed rapid excitability
444 increase in both mouse and human DRG neurons following IL-17 treatment,
445 suggesting a possible post-translational modulation of some key ion channels, such as
446 sodium channels. Our work in progress shows that IL-17 also increased sodium
447 currents (data not shown). Interestingly, we found that the enhanced excitability in
448 paclitaxel-pretreated small mouse DRG neurons can be abolished by a neutralizing
449 antibody against IL-17R antibody. Since the recordings were conducted in dissociated
450 neurons and physiological concentration of IL-17 is not present in culture medium,
451 our result suggests a possibility that IL-17R may direct regulate neuronal activity in
452 the absence of IL-17. Future study will examine how IL-17R interacts with ion
453 channels such as Nav1.7. We should not rule out the possibility that satellite glial cells
454 may also be attached to neurons in our culture conditions to communicate with
455 neurons by releasing IL-17. Our working hypothesis of peripheral glial regulation of
456 chemotherapy-evoked neuropathic pain via IL-17/IL-17R signaling is illustrated in
457 Supplementary Fig. 3.

458 ***Translational potential.*** IL-17 levels in sciatic nerves are elevated after nerve injuries
459 (Noma et al., 2011). Our data show that IL-17 levels are also elevated in CSF and
460 spinal cord in paclitaxel-treated mice. Importantly, intrathecal injection of IL-17 RA

461 antibody effectively alleviated paclitaxel-induced neuropathic pain. Chemotherapy
462 has been shown to activate cancer-associated fibroblasts to renew cancer-initiating
463 cells and maintain colorectal cancer by IL-17 secretion (Lotti et al., 2013). Thus,
464 targeting IL-17 signaling may not only alleviate neuropathic pain but also improve
465 anti-cancer efficacy after chemotherapy. The translational potential of this study is
466 enhanced by demonstrating hyperexcitability of human sensory neurons in response to
467 IL-17. IL-17 blockers have been developed for treating inflammatory diseases such as
468 psoriasis and arthritis (Kivelevitch and Menter, 2015). Brodalumab (Kyntheum®) is a
469 human anti-interleukin-17 receptor A (IL-17RA) monoclonal antibody available for
470 use in patients with moderate to severe plaque psoriasis (Blair, 2018). Since mouse
471 IL-17RA antibody is effective in suppressing neuronal hyperexcitability after
472 paclitaxel, Brodalumab could be used to treat CIPN and neuropathic pain.

473

474

475 **Acknowledgments**

476 This work was supported by grants from National Key R&D Program of China
477 (2017YFB0403803), National Natural Science Foundation of China (31420103903,
478 31771164 and 81471130), Development Project of Shanghai Peak Disciplines
479 Integrated Chinese and Western Medicine, and NIN R01 grants DE17794, DE22743,
480 and NS87988 to R.R.J.

481

482

483

484

485

486

487

488

489

490

491

492

493 **Competing interests**

494 All the authors have no competing financial interest in this study.

495

496

497

498

499

500

501

502

503

504

505

506

507

508

509

510 References

- 511 BASBAUM, A. I., BAUTISTA, D. M., SCHERRER, G. & JULIUS, D. 2009. Cellular and molecular
512 mechanisms of pain. *Cell*, 139, 267-284. doi:S0092-8674(09)01243-4
513 [pii];10.1016/j.cell.2009.09.028 [doi]
- 514 BLAIR, H. A. 2018. Brodalumab: A Review in Moderate to Severe Plaque Psoriasis. *Drugs*, 78, 495-504.
515 doi:10.1007/s40265-018-0888-4
- 516 BRAZ, J., SOLORZANO, C., WANG, X. & BASBAUM, A. I. 2014. Transmitting Pain and Itch Messages: A
517 Contemporary View of the Spinal Cord Circuits that Generate Gate Control. *Neuron*, 82,
518 522-536. doi:S0896-6273(14)00023-3 [pii];10.1016/j.neuron.2014.01.018 [doi]
- 519 CHANG, W., BERTA, T., KIM, Y. H., LEE, S., LEE, S. Y. & JI, R. R. 2017. Expression and Role of
520 Voltage-Gated Sodium Channels in Human Dorsal Root Ganglion Neurons with Special Focus
521 on Nav1.7, Species Differences, and Regulation by Paclitaxel. *Neurosci Bull.*
522 doi:10.1007/s12264-017-0132-3
- 523 CHANG, W., BERTA, T., KIM, Y. H., LEE, S., LEE, S. Y. & JI, R. R. 2018. Expression and Role of
524 Voltage-Gated Sodium Channels in Human Dorsal Root Ganglion Neurons with Special Focus
525 on Nav1.7, Species Differences, and Regulation by Paclitaxel. *Neurosci Bull*, 34, 4-12.
526 doi:10.1007/s12264-017-0132-3
- 527 CHEN, C., ITAKURA, E., NELSON, G. M., SHENG, M., LAURENT, P., FENK, L. A., BUTCHER, R. A., HEGDE, R.
528 S. & DE BONO, M. 2017. IL-17 is a neuromodulator of *Caenorhabditis elegans* sensory
529 responses. *Nature*, 542, 43-48. doi:10.1038/nature20818
- 530 CHEN, G., PARK, C. K., XIE, R. G. & JI, R. R. 2015. Intrathecal bone marrow stromal cells inhibit
531 neuropathic pain via TGF-beta secretion. *J Clin.Invest*, 125, 3226-3240. doi:80883
532 [pii];10.1172/JCI80883 [doi]
- 533 CHEN, J. T., GUO, D., CAMPANELLI, D., FRATTINI, F., MAYER, F., ZHOU, L., KUNER, R., HEPPENSTALL, P. A.,
534 KNIPPER, M. & HU, J. 2014. Presynaptic GABAergic inhibition regulated by BDNF contributes
535 to neuropathic pain induction. *Nat Commun*, 5, 5331. doi:10.1038/ncomms6331
- 536 CHIRILA, A. M., BROWN, T. E., BISHOP, R. A., BELLONO, N. W., PUCCI, F. G. & KAUER, J. A. 2014.
537 Long-term potentiation of glycinergic synapses triggered by interleukin 1beta.
538 *Proc.Natl.Acad.Sci.U.S.A*, 111, 8263-8268. doi:1401013111 [pii];10.1073/pnas.1401013111
539 [doi]
- 540 COULL, J. A., BOUDREAU, D., BACHAND, K., PRESCOTT, S. A., NAULT, F., SIK, A., DE KONINCK, P. & DE
541 KONINCK, Y. 2003. Trans-synaptic shift in anion gradient in spinal lamina I neurons as a
542 mechanism of neuropathic pain. *Nature*, 424, 938-942
- 543 DOUGHERTY, P. M., CATA, J. P., CORDELLA, J. V., BURTON, A. & WENG, H. R. 2004. Taxol-induced
544 sensory disturbance is characterized by preferential impairment of myelinated fiber function
545 in cancer patients. *Pain*, 109, 132-42. doi:10.1016/j.pain.2004.01.021
- 546 DUAN, B., CHENG, L., BOURANE, S., BRITZ, O., PADILLA, C., GARCIA-CAMPMANY, L., KRASHES, M.,
547 KNOWLTON, W., VELASQUEZ, T., REN, X., ROSS, S. E., LOWELL, B. B., WANG, Y., GOULDING, M.
548 & MA, Q. 2014a. Identification of spinal circuits transmitting and gating mechanical pain. *Cell*,
549 159, 1417-1432. doi:S0092-8674(14)01434-2 [pii];10.1016/j.cell.2014.11.003 [doi]
- 550 DUAN, B., CHENG, L., BOURANE, S., BRITZ, O., PADILLA, C., GARCIA-CAMPMANY, L., KRASHES, M.,
551 KNOWLTON, W., VELASQUEZ, T., REN, X., ROSS, S. E., LOWELL, B. B., WANG, Y., GOULDING, M.

- 552 & MA, Q. 2014b. Identification of spinal circuits transmitting and gating mechanical pain. *Cell*,
553 159, 1417-32. doi:10.1016/j.cell.2014.11.003
- 554 DUAN, B., CHENG, L. & MA, Q. 2018. Spinal Circuits Transmitting Mechanical Pain and Itch. *Neurosci*
555 *Bull*, 34, 186-193. doi:10.1007/s12264-017-0136-z
- 556 FOSSIEZ, F., DJOSSOU, O., CHOMARAT, P., FLORES-ROMO, L., AIT-YAHIA, S., MAAT, C., PIN, J. J.,
557 GARRONE, P., GARCIA, E., SAELAND, S., BLANCHARD, D., GAILLARD, C., DAS MAHAPATRA, B.,
558 ROUVIER, E., GOLSTEIN, P., BANCHEREAU, J. & LEBECQUE, S. 1996. T cell interleukin-17
559 induces stromal cells to produce proinflammatory and hematopoietic cytokines. *J Exp Med*,
560 183, 2593-603
- 561 GAFFEN, S. L. 2009. Structure and signalling in the IL-17 receptor family. *Nat Rev Immunol*, 9, 556-67.
562 doi:10.1038/nri2586
- 563 GOSSELIN, R. D., SUTER, M. R., JI, R. R. & DECOSTERD, I. 2010. Glial cells and chronic pain.
564 *Neuroscientist*, 16, 519-531. doi:1073858409360822 [pii];10.1177/1073858409360822 [doi]
- 565 GRACE, P. M., HUTCHINSON, M. R., MAIER, S. F. & WATKINS, L. R. 2014. Pathological pain and the
566 neuroimmune interface. *Nat.Rev.Immunol*. doi:nri3621 [pii];10.1038/nri3621 [doi]
- 567 GUO, W., WANG, H., WATANABE, M., SHIMIZU, K., ZOU, S., LAGRAIZE, S. C., WEI, F., DUBNER, R. & REN,
568 K. 2007. Glial-cytokine-neuronal interactions underlying the mechanisms of persistent pain.
569 *J.Neurosci*, 27, 6006-6018. doi:27/22/6006 [pii];10.1523/JNEUROSCI.0176-07.2007 [doi]
- 570 HAN, Q., KIM, Y. H., WANG, X., LIU, D., ZHANG, Z. J., BEY, A. L., LAY, M., CHANG, W., BERTA, T., ZHANG,
571 Y., JIANG, Y. H. & JI, R. R. 2016. SHANK3 Deficiency Impairs Heat Hyperalgesia and TRPV1
572 Signaling in Primary Sensory Neurons. *Neuron*. doi:10.1016/j.neuron.2016.11.007
- 573 HOT, A. & MIOSSEC, P. 2011. Effects of interleukin (IL)-17A and IL-17F in human rheumatoid arthritis
574 synoviocytes. *Ann Rheum Dis*, 70, 727-32. doi:10.1136/ard.2010.143768
- 575 HU, H. J. & GEREAU, R. W. 2003. ERK integrates PKA and PKC signaling in superficial dorsal horn
576 neurons. II. Modulation of neuronal excitability. *J.Neurophysiol*, 90, 1680-1688
- 577 HWANG, S. Y., KIM, J. Y., KIM, K. W., PARK, M. K., MOON, Y., KIM, W. U. & KIM, H. Y. 2004. IL-17 induces
578 production of IL-6 and IL-8 in rheumatoid arthritis synovial fibroblasts via NF-kappaB- and
579 PI3-kinase/Akt-dependent pathways. *Arthritis Res Ther*, 6, R120-8. doi:10.1186/ar1038
- 580 JI, R. R. 2017. Neuroinflammation and central sensitization in chronic pain. *Anesthesiology*
- 581 JI, R. R., BERTA, T. & NEDERGAARD, M. 2013. Glia and pain: Is chronic pain a gliopathy? *Pain*.
582 doi:S0304-3959(13)00330-8 [pii];10.1016/j.pain.2013.06.022 [doi]
- 583 JI, R. R., CHAMESSIAN, A. & ZHANG, Y. Q. 2016. Pain regulation by non-neuronal cells and
584 inflammation. *Science*, 354, 572-577. doi:10.1126/science.aaf8924
- 585 JIN, S. X., ZHUANG, Z. Y., WOOLF, C. J. & JI, R. R. 2003. p38 mitogen-activated protein kinase is
586 activated after a spinal nerve ligation in spinal cord microglia and dorsal root ganglion
587 neurons and contributes to the generation of neuropathic pain. *J.Neurosci*, 23, 4017-4022
- 588 KAWASAKI, Y., ZHANG, L., CHENG, J. K. & JI, R. R. 2008. Cytokine mechanisms of central sensitization:
589 distinct and overlapping role of interleukin-1beta, interleukin-6, and tumor necrosis
590 factor-alpha in regulating synaptic and neuronal activity in the superficial spinal cord.
591 *J.Neurosci*, 28, 5189-5194
- 592 KIM, C. F. & MOALEM-TAYLOR, G. 2011. Interleukin-17 contributes to neuroinflammation and
593 neuropathic pain following peripheral nerve injury in mice. *J Pain*, 12, 370-83.
594 doi:10.1016/j.jpain.2010.08.003

- 595 KIVELEVITCH, D. N. & MENTER, A. 2015. Use of brodalumab for the treatment of psoriasis and
596 psoriatic arthritis. *Immunotherapy*, 7, 323-33. doi:10.2217/imt.14.113
- 597 KLEINSCHNITZ, C., HOFSTETTER, H. H., MEUTH, S. G., BRAEUNINGER, S., SOMMER, C. & STOLL, G. 2006.
598 T cell infiltration after chronic constriction injury of mouse sciatic nerve is associated with
599 interleukin-17 expression. *Exp Neurol*, 200, 480-5. doi:10.1016/j.expneurol.2006.03.014
- 600 KORN, T., BETTELLI, E., OUKKA, M. & KUCHROO, V. K. 2009. IL-17 and Th17 Cells. *Annu Rev Immunol*,
601 27, 485-517. doi:10.1146/annurev.immunol.021908.132710
- 602 LI, Y., ADAMEK, P., ZHANG, H., TATSUI, C. E., RHINES, L. D., MROZKOVA, P., LI, Q., KOSTURAKIS, A. K.,
603 CASSIDY, R. M., HARRISON, D. S., CATA, J. P., SAPIRE, K., ZHANG, H., KENNAMER-CHAPMAN, R.
604 M., JAWAD, A. B., GHETTI, A., YAN, J., PALECEK, J. & DOUGHERTY, P. M. 2015a. The Cancer
605 Chemotherapeutic Paclitaxel Increases Human and Rodent Sensory Neuron Responses to
606 TRPV1 by Activation of TLR4. *J Neurosci*, 35, 13487-500.
607 doi:10.1523/JNEUROSCI.1956-15.2015
- 608 LI, Y., ADAMEK, P., ZHANG, H., TATSUI, C. E., RHINES, L. D., MROZKOVA, P., LI, Q., KOSTURAKIS, A. K.,
609 CASSIDY, R. M., HARRISON, D. S., CATA, J. P., SAPIRE, K., ZHANG, H., KENNAMER-CHAPMAN, R.
610 M., JAWAD, A. B., GHETTI, A., YAN, J., PALECEK, J. & DOUGHERTY, P. M. 2015b. The Cancer
611 Chemotherapeutic Paclitaxel Increases Human and Rodent Sensory Neuron Responses to
612 TRPV1 by Activation of TLR4. *J Neurosci*, 35, 13487-13500. doi:10.1523/JNEUROSCI.1956-15.2015 [pii];10.1523/JNEUROSCI.1956-15.2015 [doi]
- 614 LOTTI, F., JARRAR, A. M., PAI, R. K., HITOMI, M., LATHIA, J., MACE, A., GANTT, G. A., JR., SUKHDEO, K.,
615 DEVECCHIO, J., VASANJ, A., LEAHY, P., HJELMELAND, A. B., KALADY, M. F. & RICH, J. N. 2013.
616 Chemotherapy activates cancer-associated fibroblasts to maintain colorectal cancer-initiating
617 cells by IL-17A. *J Exp Med*, 210, 2851-72. doi:10.1084/jem.20131195
- 618 LU, Y., DONG, H., GAO, Y., GONG, Y., REN, Y., GU, N., ZHOU, S., XIA, N., SUN, Y. Y., JI, R. R. & XIONG, L.
619 2013. A feed-forward spinal cord glycinergic neural circuit gates mechanical allodynia. *J*
620 *Clin Invest*, 123, 4050-4062. doi:10.1172/JCI70026 [pii];10.1172/JCI70026 [doi]
- 621 LUO, X., FITZSIMMONS, B., MOHAN, A., ZHANG, L., TERRANDO, N., KORDASIEWICZ, H. & JI, R. R. 2017.
622 Intrathecal administration of antisense oligonucleotide against p38alpha but not p38beta
623 MAP kinase isoform reduces neuropathic and postoperative pain and TLR4-induced pain in
624 male mice. *Brain Behav Immun*. doi:10.1016/j.bbi.2017.11.007
- 625 MCMAHON, S. B. & MALCANGIO, M. 2009. Current challenges in glia-pain biology. *Neuron*, 64, 46-54.
626 doi:10.1016/j.neuron.2009.09.033 [doi]
- 627 MCNAMEE, K. E., ALZABIN, S., HUGHES, J. P., ANAND, P., FELDMANN, M., WILLIAMS, R. O. & INGLIS, J. J.
628 2011. IL-17 induces hyperalgesia via TNF-dependent neutrophil infiltration. *Pain*, 152,
629 1838-45. doi:10.1016/j.pain.2011.03.035
- 630 MELZACK, R. & WALL, P. D. 1965. Pain mechanisms: a new theory. *Science*, 150, 971-9
- 631 MENG, X., ZHANG, Y., LAO, L., SAITO, R., LI, A., BACKMAN, C. M., BERMAN, B. M., REN, K., WEI, P. K. &
632 ZHANG, R. X. 2013. Spinal interleukin-17 promotes thermal hyperalgesia and NMDA NR1
633 phosphorylation in an inflammatory pain rat model. *Pain*, 154, 294-305.
634 doi:10.1016/j.pain.2012.10.022
- 635 MILLIGAN, E. D., O'CONNOR, K. A., NGUYEN, K. T., ARMSTRONG, C. B., TWINING, C., GAYKEMA, R. P.,
636 HOLGUIN, A., MARTIN, D., MAIER, S. F. & WATKINS, L. R. 2001. Intrathecal HIV-1 envelope
637 glycoprotein gp120 induces enhanced pain states mediated by spinal cord proinflammatory

- 638 cytokines. *J.Neurosci.*, 21, 2808-2819
- 639 MIOSSEC, P. & KOLLS, J. K. 2012. Targeting IL-17 and TH17 cells in chronic inflammation. *Nat Rev Drug*
640 *Discov*, 11, 763-76. doi:10.1038/nrd3794
- 641 MIYOSHI, K., OBATA, K., KONDO, T., OKAMURA, H. & NOGUCHI, K. 2008. Interleukin-18-mediated
642 microglia/astrocyte interaction in the spinal cord enhances neuropathic pain processing after
643 nerve injury. *J.Neurosci.*, 28, 12775-12787. doi:28/48/12775
644 [pii];10.1523/JNEUROSCI.3512-08.2008 [doi]
- 645 NOMA, N., KHAN, J., CHEN, I. F., MARKMAN, S., BENOLIEL, R., HADLAQ, E., IMAMURA, Y. & ELIAV, E.
646 2011. Interleukin-17 levels in rat models of nerve damage and neuropathic pain. *Neurosci*
647 *Lett*, 493, 86-91. doi:10.1016/j.neulet.2011.01.079
- 648 PARK, C. K., LU, N., XU, Z. Z., LIU, T., SERHAN, C. N. & JI, R. R. 2011. Resolving TRPV1- and
649 TNF- α -mediated spinal cord synaptic plasticity and inflammatory pain with neuroprotectin
650 D1. *J Neurosci*, 31, 15072-15085. doi:31/42/15072 [pii];10.1523/JNEUROSCI.2443-11.2011
651 [doi]
- 652 PINTO, L. G., CUNHA, T. M., VIEIRA, S. M., LEMOS, H. P., VERRI, W. A., JR., CUNHA, F. Q. & FERREIRA, S.
653 H. 2010. IL-17 mediates articular hypernociception in antigen-induced arthritis in mice. *Pain*,
654 148, 247-56. doi:10.1016/j.pain.2009.11.006
- 655 POLOMANO, R. C., MANNES, A. J., CLARK, U. S. & BENNETT, G. J. 2001. A painful peripheral neuropathy
656 in the rat produced by the chemotherapeutic drug, paclitaxel. *Pain*, 94, 293-304
- 657 REN, K. & DUBNER, R. 2010. Interactions between the immune and nervous systems in pain. *Nat.Med.*,
658 16, 1267-1276. doi:nm.2234 [pii];10.1038/nm.2234 [doi]
- 659 RICHTER, F., NATURA, G., EBBINGHAUS, M., VON BANCHET, G. S., HENSELLEK, S., KONIG, C., BRAUER, R.
660 & SCHAIBLE, H. G. 2012. Interleukin-17 sensitizes joint nociceptors to mechanical stimuli and
661 contributes to arthritic pain through neuronal interleukin-17 receptors in rodents. *Arthritis*
662 *Rheum*, 64, 4125-34. doi:10.1002/art.37695
- 663 SEGOND VON BANCHET, G., BOETTGER, M. K., KONIG, C., IWAKURA, Y., BRAUER, R. & SCHAIBLE, H. G.
664 2013. Neuronal IL-17 receptor upregulates TRPV4 but not TRPV1 receptors in DRG neurons
665 and mediates mechanical but not thermal hyperalgesia. *Mol Cell Neurosci*, 52, 152-60.
666 doi:10.1016/j.mcn.2012.11.006
- 667 SISIGNANO, M., BARON, R., SCHOLICH, K. & GEISLINGER, G. 2014. Mechanism-based treatment for
668 chemotherapy-induced peripheral neuropathic pain. *Nat Rev Neurol*, 10, 694-707.
669 doi:10.1038/nrneurol.2014.211
- 670 SOMMER, C. 1999. [Animal studies on neuropathic pain: the role of cytokines and cytokine receptors
671 in pathogenesis and therapy]. *Schmerz.*, 13, 315-323
- 672 SOUTH, S. M., KOHNO, T., KASPAR, B. K., HEGARTY, D., VISSSEL, B., DRAKE, C. T., OHATA, M., JENAB, S.,
673 SAILER, A. W., MALKMUS, S., MASUYAMA, T., HORNER, P., BOGULAVSKY, J., GAGE, F. H., YAKSH,
674 T. L., WOOLF, C. J., HEINEMANN, S. F. & INTURRISI, C. E. 2003. A conditional deletion of the
675 NR1 subunit of the NMDA receptor in adult spinal cord dorsal horn reduces NMDA currents
676 and injury-induced pain. *J Neurosci*, 23, 5031-40
- 677 SWEITZER, S. M., COLBURN, R. W., RUTKOWSKI, M. & DELEO, J. A. 1999. Acute peripheral
678 inflammation induces moderate glial activation and spinal IL-1beta expression that correlates
679 with pain behavior in the rat. *Brain Res.*, 829, 209-221
- 680 TAKAZAWA, T., CHOUDHURY, P., TONG, C. K., CONWAY, C. M., SCHERRER, G., FLOOD, P. D., MUKAI, J. &

- 681 MACDERMOTT, A. B. 2017. Inhibition Mediated by Glycinergic and GABAergic Receptors on
682 Excitatory Neurons in Mouse Superficial Dorsal Horn Is Location-Specific but Modified by
683 Inflammation. *J Neurosci*, 37, 2336-2348. doi:10.1523/JNEUROSCI.2354-16.2017
- 684 TODD, A. J. 2010. Neuronal circuitry for pain processing in the dorsal horn. *Nat.Rev.Neurosci.*, 11,
685 823-836. doi:nrn2947 [pii];10.1038/nrn2947 [doi]
- 686 WALL, P. D. 1978. The gate control theory of pain mechanisms. A re-examination and re-statement.
687 *Brain*, 101, 1-18
- 688 WOOLF, C. J. & SALTER, M. W. 2000. Neuronal plasticity: increasing the gain in pain. *Science*, 288,
689 1765-1769
- 690 WOOLF, C. J. & THOMPSON, S. W. 1991. The induction and maintenance of central sensitization is
691 dependent on N-methyl-D-aspartic acid receptor activation; implications for the treatment of
692 post-injury pain hypersensitivity states. *Pain*, 44, 293-9
- 693 XIE, R. G., GAO, Y. J., PARK, C. K., LU, N., LUO, C., WANG, W. T., WU, S. X. & JI, R. R. 2018. Spinal CCL2
694 Promotes Central Sensitization, Long-Term Potentiation, and Inflammatory Pain via CCR2:
695 Further Insights into Molecular, Synaptic, and Cellular Mechanisms. *Neurosci Bull*, 34, 13-21.
696 doi:10.1007/s12264-017-0106-5
- 697 XU, Z. Z., KIM, Y. H., BANG, S., ZHANG, Y., BERTA, T., WANG, F., OH, S. B. & JI, R. R. 2015. Inhibition of
698 mechanical allodynia in neuropathic pain by TLR5-mediated A-fiber blockade. *Nat Med*, 21,
699 1326-31. doi:10.1038/nm.3978
- 700 XU, Z. Z., LIU, X. J., BERTA, T., PARK, C. K., LU, N., SERHAN, C. N. & JI, R. R. 2013.
701 Neuroprotectin/protectin D1 protects against neuropathic pain in mice after nerve trauma.
702 *Ann Neurol*, 74, 490-5. doi:10.1002/ana.23928
- 703 XU, Z. Z., ZHANG, L., LIU, T., PARK, J. Y., BERTA, T., YANG, R., SERHAN, C. N. & JI, R. R. 2010. Resolvins
704 RvE1 and RvD1 attenuate inflammatory pain via central and peripheral actions. *Nat.Med.*, 16,
705 592-7, 1p. doi:nm.2123 [pii];10.1038/nm.2123 [doi]
- 706 YANG, Y., LI, H., LI, T. T., LUO, H., GU, X. Y., LU, N., JI, R. R. & ZHANG, Y. Q. 2015. Delayed Activation of
707 Spinal Microglia Contributes to the Maintenance of Bone Cancer Pain in Female Wistar Rats
708 via P2X7 Receptor and IL-18. *J.Neurosci.*, 35, 7950-7963. doi:35/20/7950
709 [pii];10.1523/JNEUROSCI.5250-14.2015 [doi]
- 710 ZEILHOFER, H. U., BENKE, D. & YEVENES, G. E. 2012a. Chronic pain states: pharmacological strategies
711 to restore diminished inhibitory spinal pain control. *Annu.Rev.Pharmacol.Toxicol.*, 52, 111-133.
712 doi:10.1146/annurev-pharmtox-010611-134636 [doi]
- 713 ZEILHOFER, H. U., WILDNER, H. & YEVENES, G. E. 2012b. Fast synaptic inhibition in spinal sensory
714 processing and pain control. *Physiol Rev*, 92, 193-235. doi:10.1152/physrev.00043.2010
- 715 ZELENKA, M., SCHAFERS, M. & SOMMER, C. 2005. Intraneural injection of interleukin-1beta and tumor
716 necrosis factor-alpha into rat sciatic nerve at physiological doses induces signs of neuropathic
717 pain. *Pain*, 116, 257-263. doi:S0304-3959(05)00188-0 [pii];10.1016/j.pain.2005.04.018 [doi]
- 718 ZHANG, H. & DOUGHERTY, P. M. 2014. Enhanced excitability of primary sensory neurons and altered
719 gene expression of neuronal ion channels in dorsal root ganglion in paclitaxel-induced
720 peripheral neuropathy. *Anesthesiology*, 120, 1463-75. doi:10.1097/ALN.0000000000000176
- 721 ZHANG, H., NEI, H. & DOUGHERTY, P. M. 2010. A p38 mitogen-activated protein kinase-dependent
722 mechanism of disinhibition in spinal synaptic transmission induced by tumor necrosis
723 factor-alpha. *J.Neurosci.*, 30, 12844-12855. doi:30/38/12844

724 [pii];10.1523/JNEUROSCI.2437-10.2010 [doi]
725 ZHANG, H., YOON, S. Y., ZHANG, H. & DOUGHERTY, P. M. 2012a. Evidence that spinal astrocytes but
726 not microglia contribute to the pathogenesis of Paclitaxel-induced painful neuropathy. *J Pain*,
727 13, 293-303. doi:10.1016/j.jpain.2011.12.002
728 ZHANG, H., YOON, S. Y., ZHANG, H. & DOUGHERTY, P. M. 2012b. Evidence that spinal astrocytes but
729 not microglia contribute to the pathogenesis of Paclitaxel-induced painful neuropathy. *J.Pain*,
730 13, 293-303. doi:S1526-5900(11)00933-3 [pii];10.1016/j.jpain.2011.12.002 [doi]

731

732

733

734

735

736

737

738

739

740

741

742

743

744

745 **Figures and figure legends**

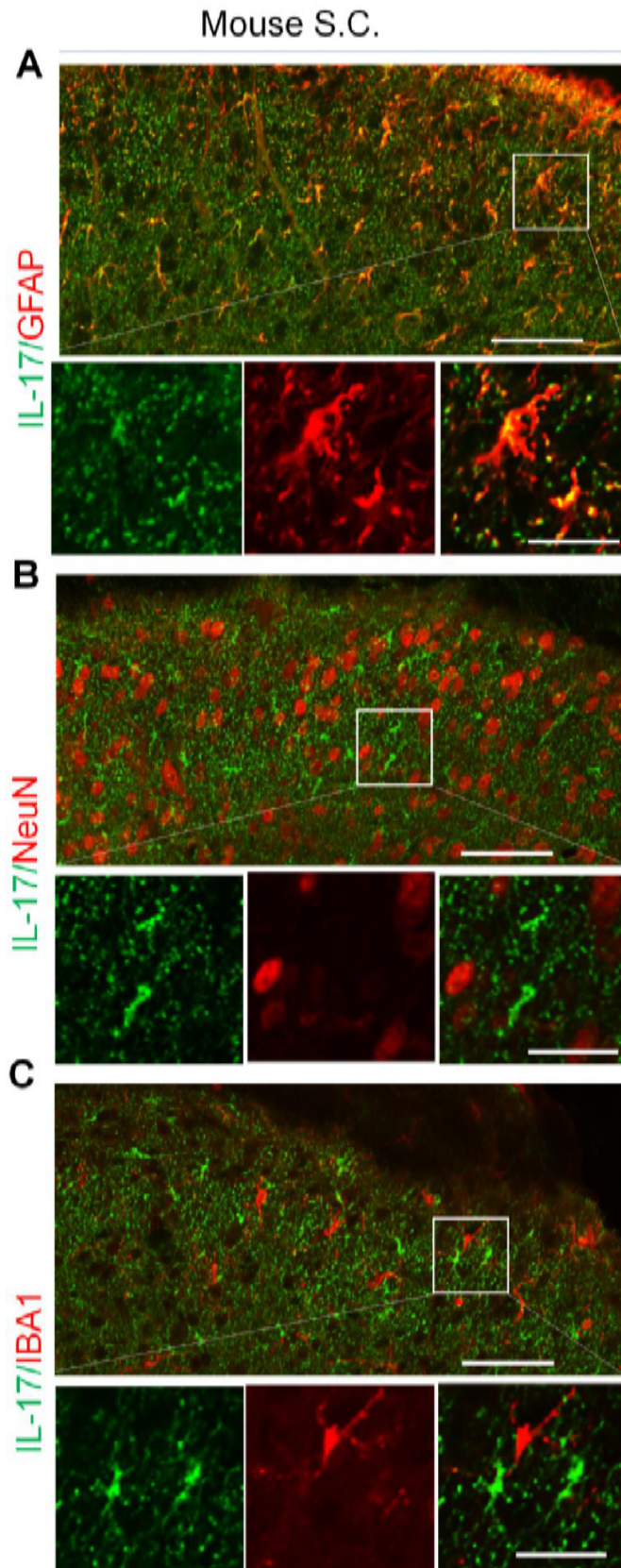


Figure 1. Photomicrographs showing IL-17 expression and colocalization of IL-17 with GFAP in spinal dorsal horn (SDH). Double labeling of IL-17 with astrocyte marker GFAP (A), neuron marker NeuN (B), and microglia marker IBA1 (C) in SDH. The white square in the top image is enlarged in three separate boxes with single and merged images in each picture (A, B and C). The scale bars represent 50 μ m (top) and 20 μ m (bottom).

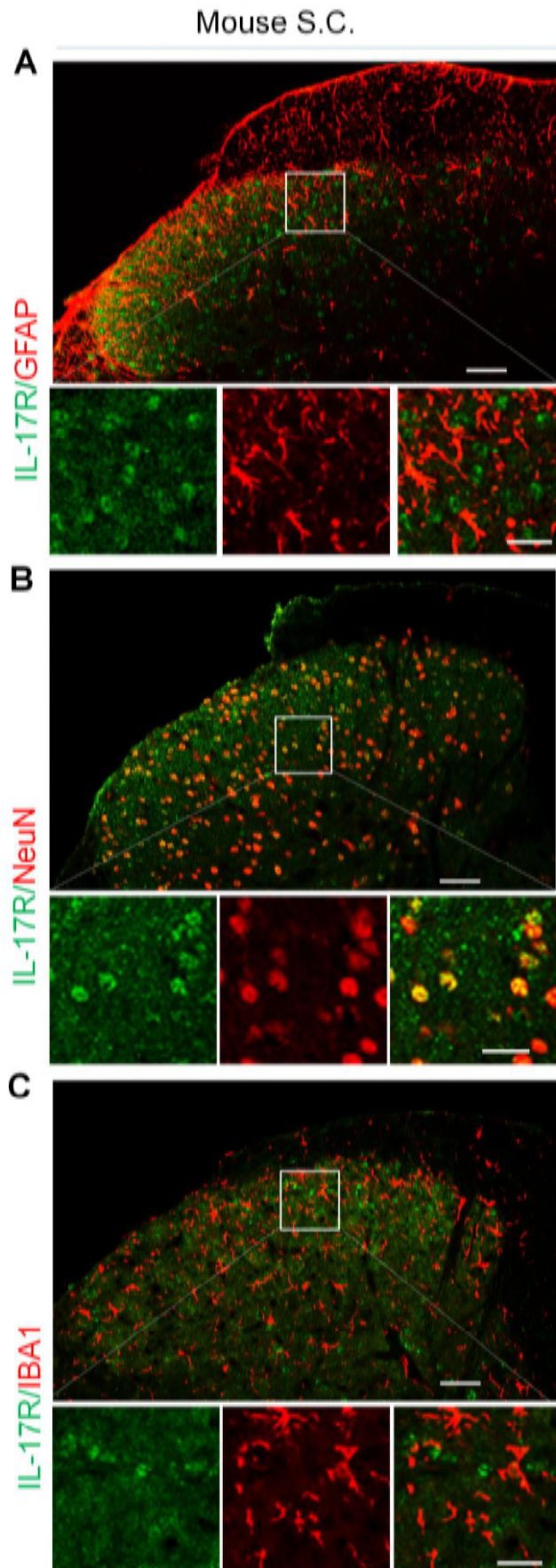
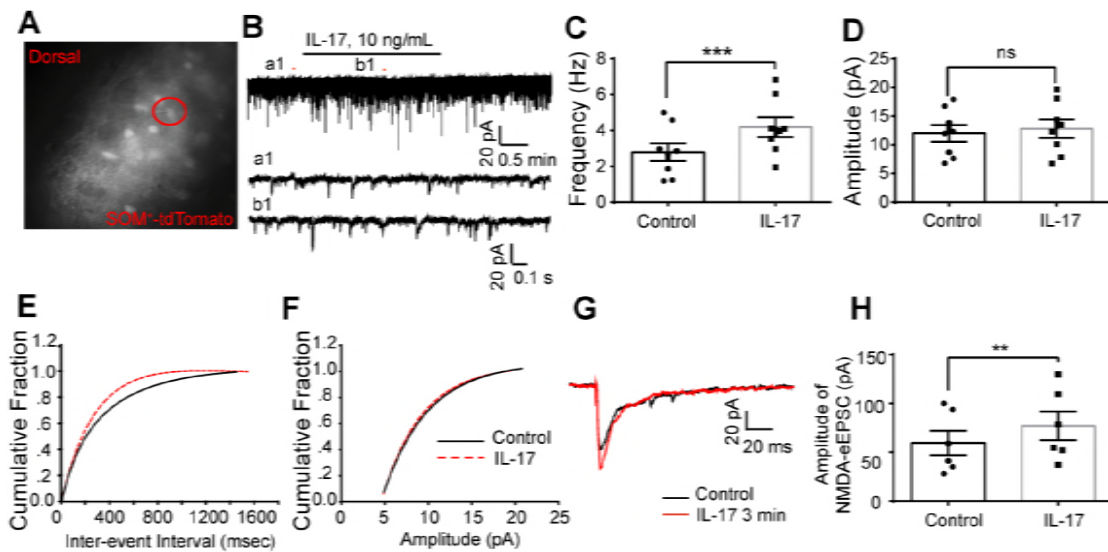


Figure 2. Photomicrographs showing IL-17 receptor (IL-17R) expression and colocalization of IL-17R with NeuN in SDH. Double labeling of IL-17R with astrocyte marker GFAP (A), neuron marker NeuN (B), and microglia marker IBA1 (C) in SDH. The white square in the top image is enlarged in three separate boxes with single and merged images in each picture (A, B and C). The scale bars represent 50 μ m (top) and 20 μ m (bottom).

795



796

797 **Figure 3. Potentiation of excitatory synaptic transmission by IL-17 in SDH**
798 **lamina II_o SOM⁺ neurons.** (A) Mouse spinal cord slice image showing a recording
799 electrode in a SOM⁺ neuron (red circle). (B) Traces of sEPSCs in lamina II_o SOM⁺
800 neurons after perfusion of IL-17 (10 ng/mL, 2 min). a1 and b1 are enlargements of the
801 recordings before and after IL-17 treatment, respectively. (C, D) Quantification of
802 changes in frequency and amplitude of sEPSCs (n=8 neurons/group). (E, F)
803 Corresponding cumulative distributions of inter-event interval and amplitude from
804 one neuron. (G) Traces of NMDA-eEPSC before (black) and after (red) IL-17
805 treatment. (H) Potentiation of the amplitude of NMDA-eEPSC by IL-17 (n=6). **
806 P<0.01, ***P<0.001, two-tailed paired student's test. ns, not significant. All the data
807 were mean ± S.E.M.

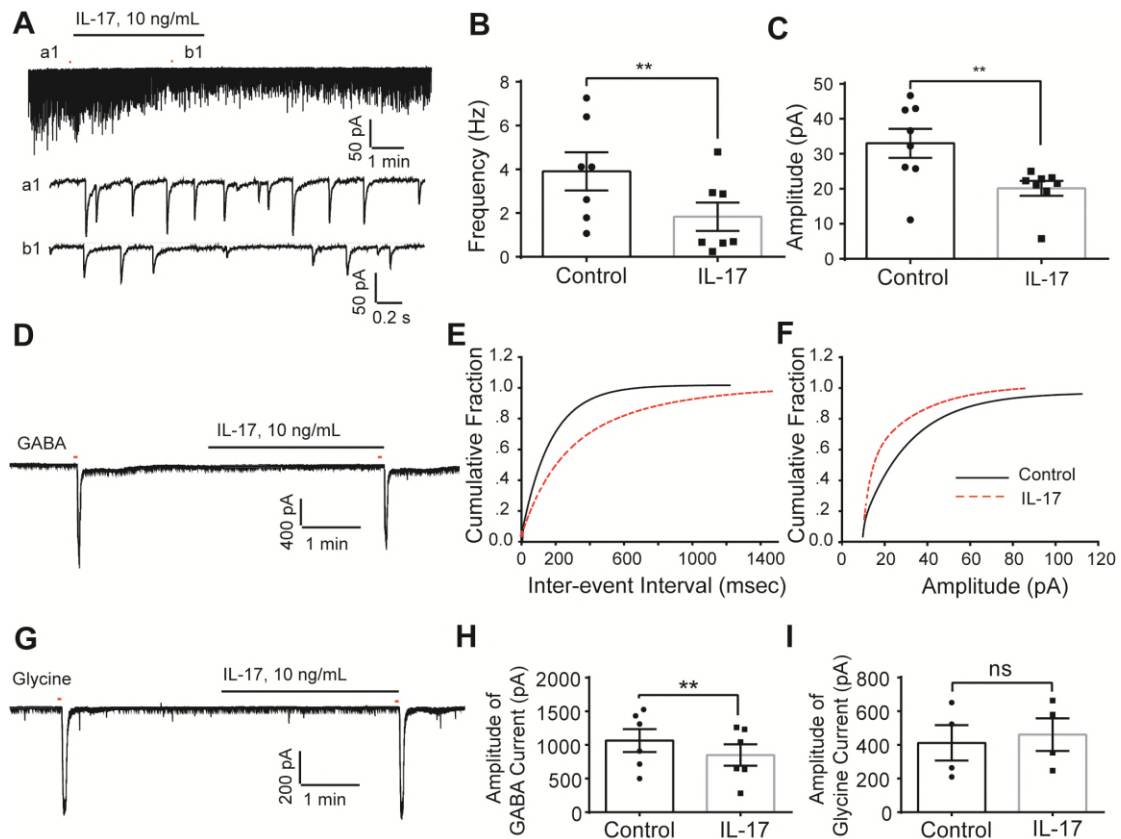
808

809

810

811

812

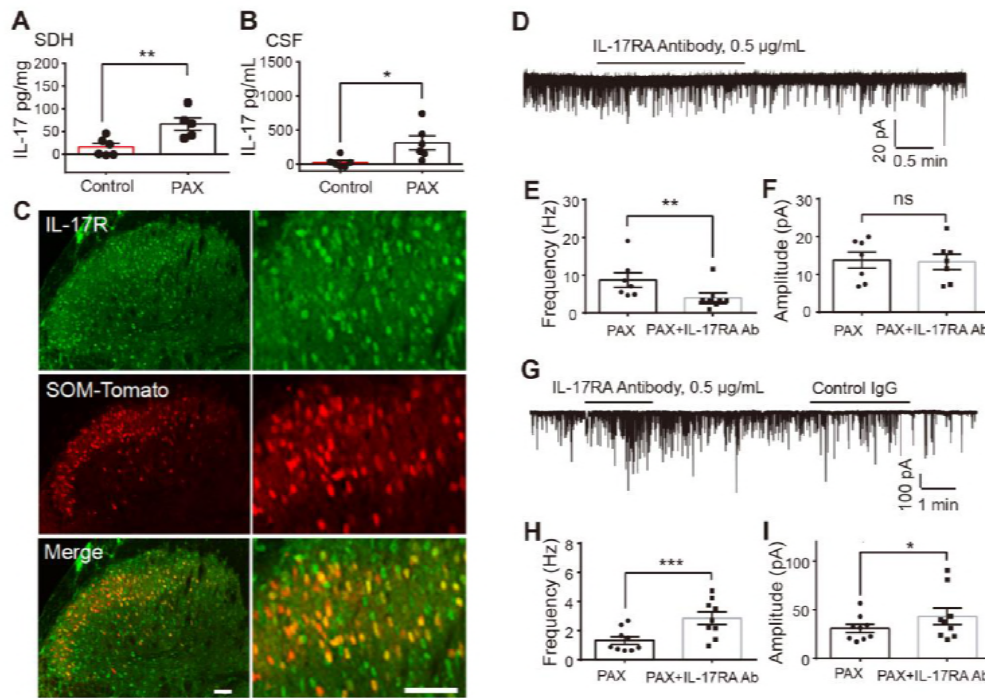


813

814 **Figure 4. Suppression of inhibitory synaptic transmission in SOM⁺ excitatory**
 815 **neurons by IL-17 in spinal cord slices.** (A) Typical traces of sIPSC in lamina II
 816 SOM⁺ neurons after perfusion of IL-17 (10 ng/mL, 2 min). a1 and b1 are
 817 enlargements of the recordings before and after IL-17 treatment, respectively. (B, C)
 818 Quantification of changes in frequency and amplitude of sIPSC (n=7, neurons/group).
 819 (D) Traces of GABA-induced current before (left) and after (right) IL-17 treatment.
 820 100 μ M GABA was applied for 3 seconds to induce an inward current. (E, F)
 821 Corresponding cumulative distributions of inter-event interval and amplitude from
 822 one neuron. (G) Traces of glycine-induced current before (left) and after (right) IL-17
 823 treatment. 1 mM glycine was applied for 3 seconds to induce an inward current. (H)
 824 Suppression of the amplitude of GABA-induced current by IL-17 (n=6
 825 neurons/group). (I) No changes in the amplitude of glycine-induced current by IL-17
 826 (n=4). ** P<0.01, two-tailed paired student's test. ns, not significant. All the data were
 827 mean \pm S.E.M.

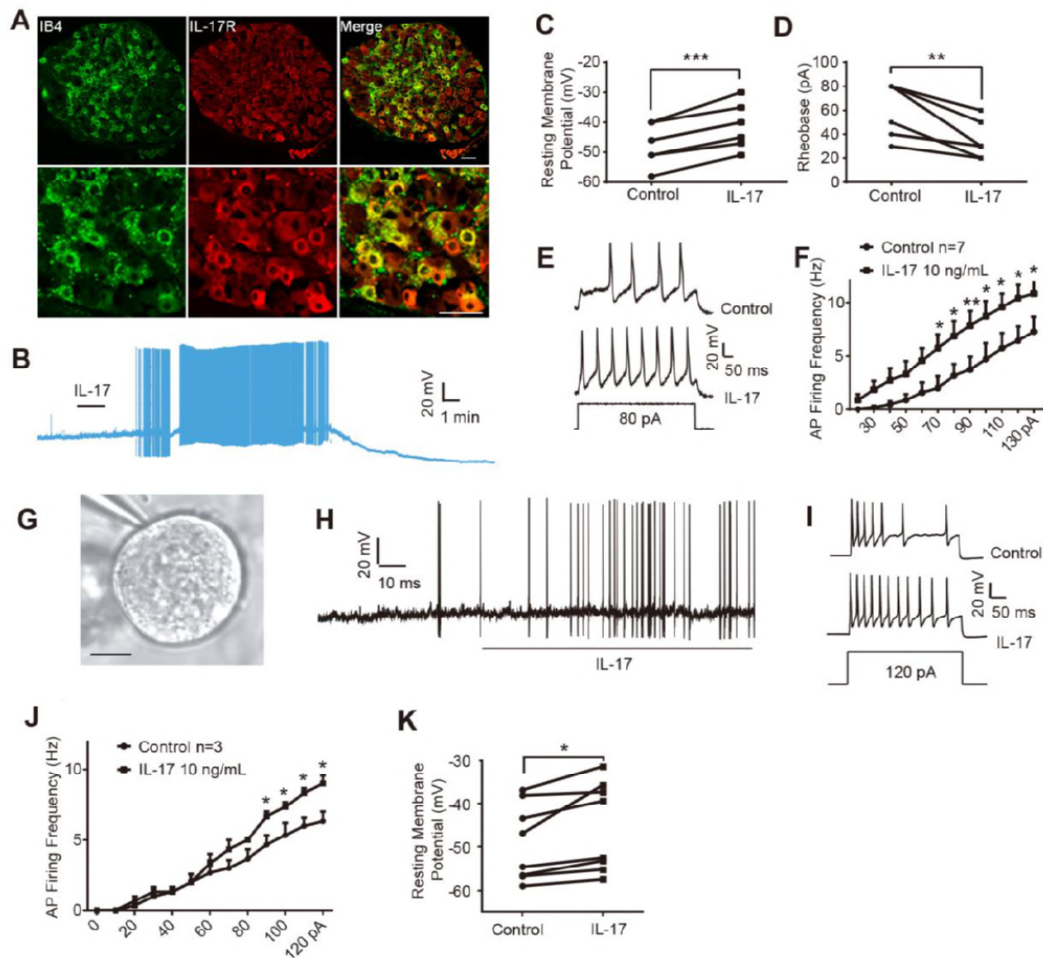
828

829



830

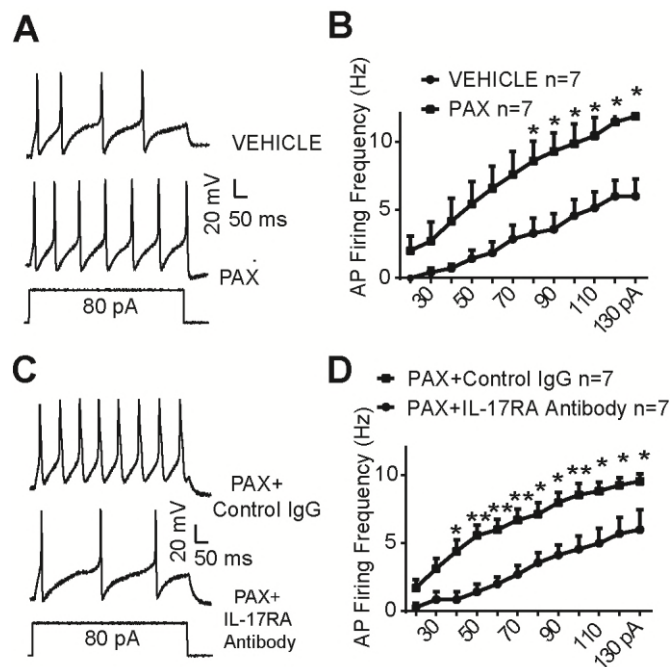
831 **Figure 5. Endogenous IL-17 regulates synaptic transmission in paclitaxel-treated**
832 **mice via IL-17R.** (A, B) ELISA analysis showing IL-17 levels in SDH (A) and CSF
833 (B) samples of control and paclitaxel treated mice. The samples were collected 7 d
834 after the paclitaxel treatment. * $P < 0.05$, ** $P < 0.01$, two-tailed unpaired student's test.
835 $n = 6$ animals/group. Sample sizes are indicated in each graph. (C) IL-17R expression
836 in SOM^+ neurons in SDH. Scale bar: $50 \mu m$. (D) Traces of sEPSCs in lamina IIo
837 SOM^+ neurons following paclitaxel treatment before and after perfusion of IL-17
838 receptor A antibody (IL-17RA Ab, $0.5 \mu g/mL$, 2 min). (E, F) Quantification of change
839 in frequency and amplitude of sEPSCs ($n = 7$). (G) Typical Traces of sIPSC in lamina
840 II SOM^+ neurons 7 days following paclitaxel treatment before and after perfusion of
841 IL-17RA Ab ($0.5 \mu g/mL$, 2 min). (H, I) Quantification of changes in frequency and
842 amplitude of sIPSC ($n = 9$). * $P < 0.05$, ** $P < 0.01$, *** $P < 0.001$, two-tailed paired
843 student's test. ns, not significant. All the data were mean \pm S.E.M.



844

845 **Figure 6. IL-17 increases the excitability of dissociated mouse DRG (mDRG) and**
 846 **human DRG neurons. (A)** IL-17R expression in mDRG neurons. Scale bar: 50 μ m.
 847 **(B)** Acute application of IL-17 (10 ng/mL) evoked spontaneous action potentials (APs)
 848 in mDRG neurons. **(C, D)** The effects of IL-17 on resting membrane potential **(C)** and
 849 rheobase **(D)**. ** $P < 0.01$, *** $P < 0.001$, two-tailed paired student's test; $n = 6$
 850 neurons/group. **(E)** Traces of APs in small-sized mDRG neurons before and after
 851 perfusion of IL-17. **(F)** Quantification of firing frequency of action potentials as
 852 shown in e. * $p < 0.05$, ** $P < 0.01$; two-way ANOVA; $n = 7$ neurons/group. **(G-J)**
 853 Whole-cell recording in dissociated small-diameter ($< 55 \mu$ m) human DRG neurons.
 854 **(G)** Image of an isolated human DRG neuron with the tip of a pipette during patch
 855 clamp recording. Scale bar: 20 μ m. **(H, I)** The representative traces of action
 856 potentials. **(H)** Acute application of IL-17 (10 ng/mL) evoked spontaneous APs in a
 857 human DRG neurons. **(I)** Representative AP waveforms for the neuron **(G)** evoked by
 858 direct current injection before and after 2 min of acute perfusion with IL-17. **(J)**
 859 Quantification of firing frequency of action potentials. * $P < 0.05$, ** $P < 0.01$; two-way
 860 ANOVA; $n = 3$ neurons. **(K)** Quantification of RMPs before and after IL-17 treatment
 861 (10 ng/mL). * $P < 0.05$, ** $P < 0.01$; paired t-test; $n = 8$ neurons.

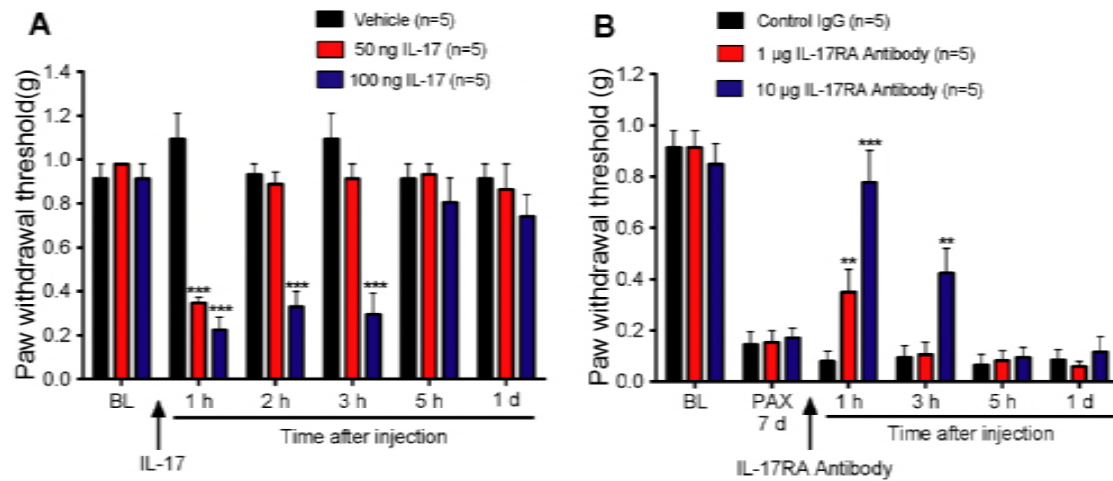
862



863

864 **Figure 7. IL-17 Receptor A neutralizing antibody inhibits the hyperexcitability of**
865 **small-sized mouse DRG (mDRG) neurons following paclitaxel treatment. (A)**
866 **Traces of APs in mDRG neurons evoked by direct current injection pretreated with**
867 **vehicle or 1 μ M paclitaxel for 3 h. (B) Quantification of APs firing frequency**
868 **pretreated with vehicle or paclitaxel. * $p < 0.05$; two-way ANOVA; and $n = 7$**
869 **neurons/group. (C) Traces of APs after application of Control IgG or IL-17RA Ab**
870 **(0.5 μ g/mL, 2 min) in paclitaxel pretreated mDRG neurons. (D) Quantification of APs**
871 **firing frequency as shown in D. * $p < 0.05$, ** $P < 0.01$; two-way ANOVA; and $n = 7$**
872 **neurons.**

873



874

875 **Figure 8. IL-17 and IL-17 receptor A (IL-17RA) contribute to paclitaxel-induced**
876 **neuropathic pain.** (A) Intrathecal injection of IL-17 induces a transient and
877 dose-dependent mechanical allodynia (i.e. reduction in PWT). (B) Mechanical
878 allodynia, induced by paclitaxel (6 mg/kg, i.p.), is attenuated by intrathecal injection
879 of IL-17RA Antibody (1 and 10 µg). * P < 0.05; **P < 0.01; ***P < 0.001; vs. control
880 IgG (10 µg, i.t.), two-way ANOVA; n = 5 mice/group.

881

882

883

884

885

886

887

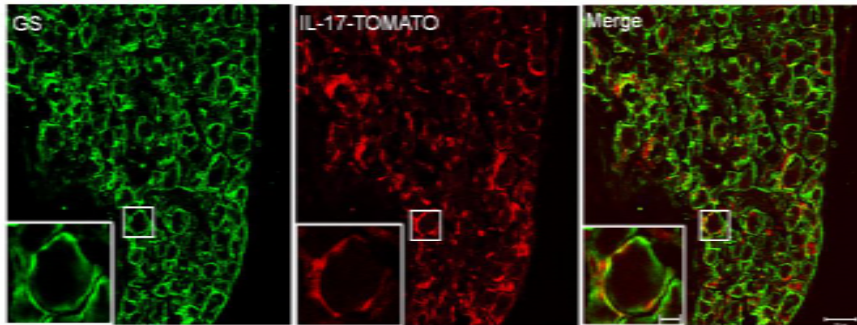
888

889

890

891

892 **Supplementary Figure 1**



893

894 **S1. Colocalization of IL-17 (red) with satellite glial marker glutamine synthetase**

895 (GS, green). Scale bar: 50 μm . The inserts are enlarged images. Scale bar: 10 μm .

896

897

898

899

900

901

902

903

904

905

906

907

908

909

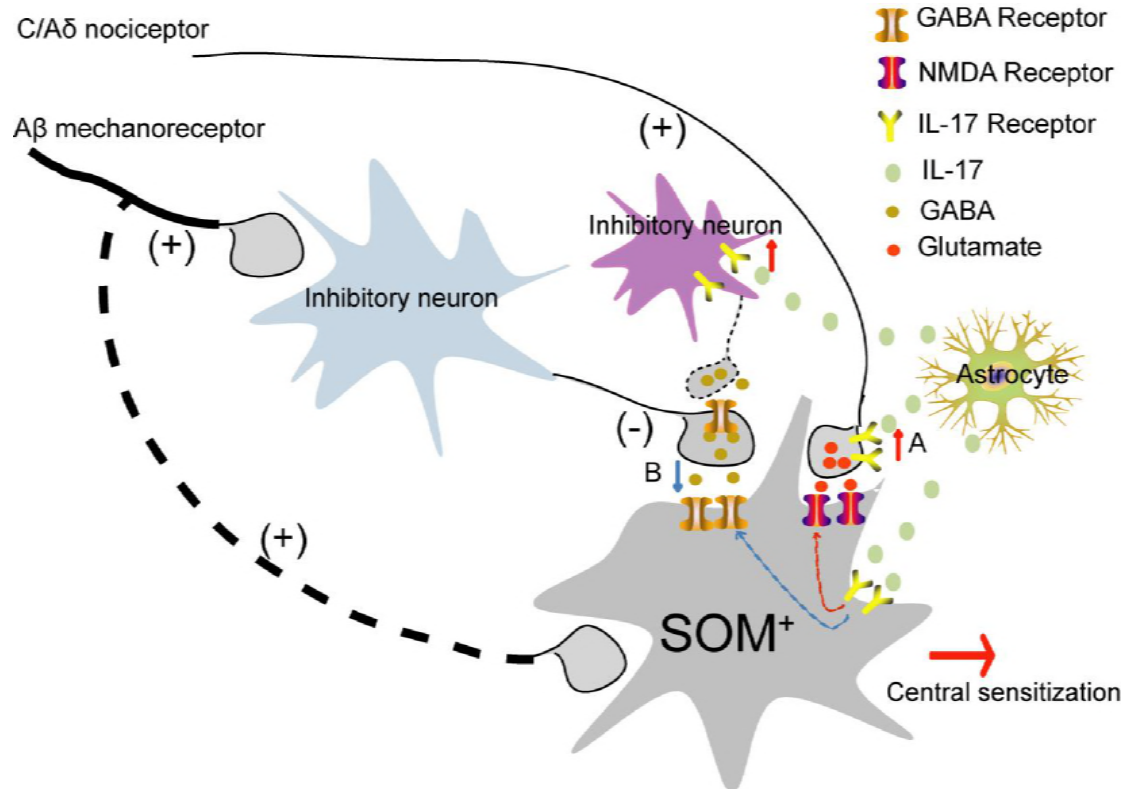
910

911

912

913 **Supplementary Figure 2**

914



915

916 **S2. A schematic showing how IL-17 modulates excitatory synaptic transmission**

917 **(A) and inhibitory synaptic transmission (B) in spinal SOM^+ neurons to induce**

918 **central sensitization and pain hypersensitivity . (A) IL-17 is released from**

919 **activated astrocytes and acts on IL-17R on presynaptic terminals and postsynaptic**

920 **SOM^+ . Activation of presynaptic IL-17R results in increased glutamate release,**

921 **whereas activation of postsynaptic IL-17R also enhances NMDAR activity.**

922 **(B) IL-17 is also expressed by inhibitory neurons and facilitates GABA release to**

923 **inhibit an inhibitory neuron, leading to a reduction in presynaptic inhibitory control of**

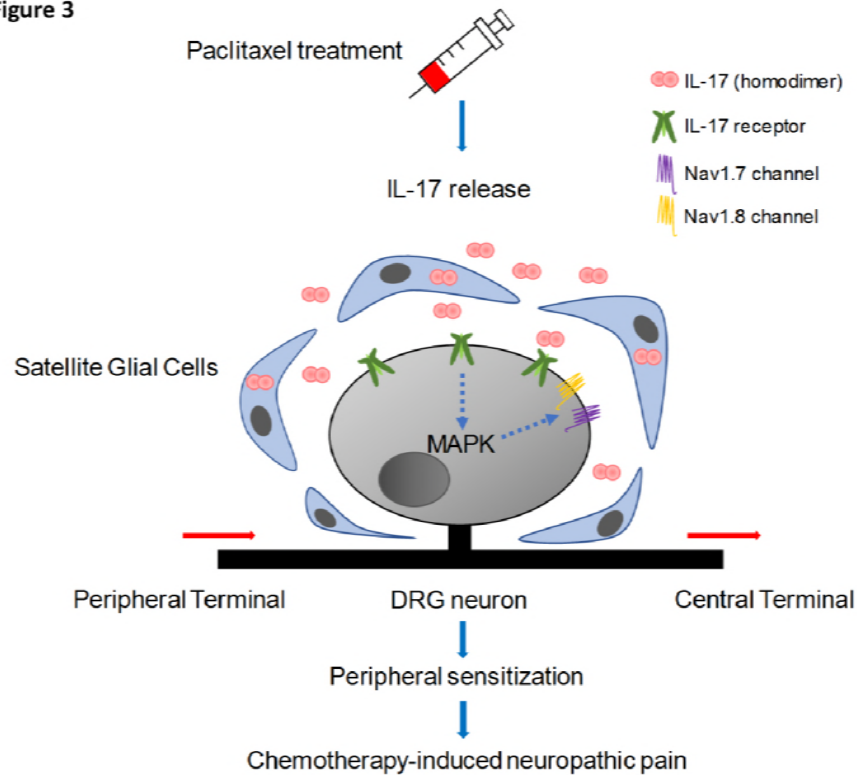
924 **spinal SOM^+ neurons. This disinhibition will also cause hyperactivity in SOM^+**

925 **neurons.**

926

927 **Supplementary Figure 3**

Supplementary Figure 3



928

929 **S3.** A schematic showing IL-17-induced neuron-glia interaction in DRG. IL-17 is
930 expressed by satellite glial cells. Following chemotherapy, IL-17 released from
931 satellite glia acts on IL-17R on nociceptive neurons to increase neuronal excitability
932 and induce peripheral sensitization.

933

934

935